Applied Physics Letters

Electric field- and strain-induced bandgap modulation in bilayer C_2N

Cite as: Appl. Phys. Lett. **120**, 203101 (2022); https://doi.org/10.1063/5.0093060
Submitted: 25 March 2022 • Accepted: 04 May 2022 • Published Online: 16 May 2022

Klichchupong Dabsamut, Tosapol Maluangnont, Pakpoom Reunchan, et al.

View Online Export Citation CrossMark

Lock-in Amplifiers up to 600 MHz
Zurich Instruments
Watch



AIP Publishing

© 2022 Author(s).

Applied Physics Letters ARTICLE scitation.org/journal/apl

Electric field- and strain-induced bandgap modulation in bilayer C_2N

Cite as: Appl. Phys. Lett. **120**, 203101 (2022); doi: 10.1063/5.0093060
Submitted: 25 March 2022 · Accepted: 4 May 2022 ·
Published Online: 16 May 2022

View Online Export Citation CrossMark

Klichchupong Dabsamut,[1,2] Tosapol Maluangnont,[3] Pakpoom Reunchan,[1] Jiraroj T-Thienprasert,[1] Sirichok Jungthawan,[4] and Adisak Boonchun[1,a)]

AFFILIATIONS

[1]Department of Physics, Faculty of Science, Kasetsart University, Bangkok 10900, Thailand
[2]Department of Physics, Case Western Reserve University, 10900 Euclid Avenue, Cleveland, Ohio 44106-7079, USA
[3]Electroceramics Research Laboratory, College of Materials Innovation and Technology, King Mongkut's Institute of Technology Ladkrabang,
Bangkok 10520, Thailand
[4]School of Physics, Institute of Science, and Center of Excellence in Advanced Functional Materials,
Suranaree University of Technology, Nakhon Ratchasima 30000, Thailand

[a)]**Author to whom correspondence should be addressed:** adisak.bo@ku.th

ABSTRACT

Recently, the C_2N monolayer with an optical bandgap of 1.96 eV has emerged as a novel two-dimensional material for modern optoelectronic devices. Herein, we report its bandgap modulation by using a simple bilayer formation that includes the application of an electric field and strain. We identify four energetically favorable bilayer configurations (AA-, AB-, AB′-, and Min-stacking) by using a hybrid functional, obtaining a calculated bandgap of 1.3–1.6 eV. When subjected to a perpendicular electric field up to 4 V/nm, the bandgap decreases by as much as 0.5 eV, which correlates with the increasing energy of the valence-band maximum, where the N-p_x and N-p_y states shift closer to the N-p_z state. Without the electric field, the bandgap decreases when the interlayer distance is contracted by a compressive strain. We express the strain (or interlayer distance) and the physical applied pressure via the stabilized jellium equation of state. For the Min-stacking configuration, the bandgap decreases from 1.75 to 0.9 eV upon applying a pressure of 35 GPa. The strain-induced reduction in the bandgap is similarly monitored under an applied electric field. Our theoretical work suggests that the electric field and strain (or applied pressure) can be used to tune the electronic properties of the bilayer C_2N.

Published under an exclusive license by AIP Publishing. https://doi.org/10.1063/5.0093060

Given that graphene's zero bandgap somewhat restricts the application of this material, several solutions for precisely tuning the bandgap have been studied, including strain engineering via deposition onto a substrate,[1] applying an external stress,[2] changing the morphology to nanoribbons,[3] doping with foreign elements such as hydrogen[4] or nitrogen,[5] forming a bilayer with different configurations,[6–8] and breaking the electrical symmetry.[9] These potential modifications have been similarly applied to other two-dimensional (2D) materials such as hexagonal boron nitride,[10] phosphorene,[11] and transition-metal dichalcogenides.[12]

C_2N monolayers have experimentally emerged as a novel 2D material with a graphene-like nitrogenated holey structure.[13] C_2N possesses an optical bandgap of 1.96 eV, which is suitable for photocatalysis and use in optoelectronic devices, and numerous theoretical and experimental studies are available that describe the physical properties of C_2N monolayers, bilayers, or few-layers. The bandgap of C_2N monolayers does not change when exposed to an external electric field. Zhang *et al.*[14] investigated the electronic structure of few-layer C_2N under a vertical applied electric field by using a standard Heyd-Scuseria-Ernzerhof (HSE) hybrid functional. The HSE bandgap of 2.47 eV (Ref. 14) is much greater than the experimental value of 1.96 eV.[13] In contrast with the monolayer, the bandgap of few-layer C_2N monotonically decreases with increasing electric field.

Zhang *et al.*[14] previously elucidated the structure and stability of bilayer C_2N in three high-symmetry arrangements (AA-, AB-, and AB′-stacking). In AA-stacking, the upper layer is placed exactly over the bottom layer. In AB stacking, the upper layer glides along the zigzag path by $\vec{a}/3 - \vec{b}/3$, where a and b are unit-cell translation vectors. For AB′ stacking, the top layer glides by $\vec{a}/2$ along the armchair direction. Interestingly, Longuinhos and Ribeiro-Soares[15] report that the AB configuration studied by Zhang *et al.*[14] is not the most energetically favorable structure. Instead, several low-symmetry structures

Published under an exclusive license by AIP Publishing

where the two layers shift slightly from the AB configuration are among the most stable structures. More recently, we examined the energy landscape of the bilayer configurations in C_2N[16] and found the six most stable arrangements moving from the simple AB configuration. These arrangements are called Min-stacking.

Density-functional theory (DFT) has proven to be an efficient method for providing precise guidance for experimentation[17,18] and for understanding the structural and electrical characteristics of 2D nanosheets, particularly their stacking sequence. Here, we report first-principles DFT calculations on the bandgap modulation of different bilayer C_2N configurations under an external electric field and applied tensile or compressive strain. The bandgap decreases as the electric-field strength increases. Moreover, the effect of strain applied perpendicularly to the plane with and without electric field is investigated. Unlike graphene, the results indicate that the bandgap can be modulated via strain engineering without applying an electric field. The perpendicular stain to the plane (interlayer distance) is related to the applied pressure,[19] suggesting that this is a potential bandgap-modulation method that should be experimentally validated.

DFT is implemented by using the Vienna *ab initio* simulation package.[20,21] The core electrons are handled by using the projector-augmented wave technique.[22] The optimal lattice parameter and band structures were estimated by using HSE with $\alpha = 0.05$ to provide a more accurate description of the electronic states. This mixing parameter exactly matches the measured bandgap of monolayer C_2N. The plane wave expansions have a kinetic energy cutoff of 520 eV. The gamma-centered $3 \times 3 \times 1$ k-point sampling is adopted. A 36-atom C_2N unit cell was used in the total-energy calculations. To eliminate interactions between two neighboring periodic patterns, a vacuum region of 20 Å was employed. Electronic and structural relaxations were carried out until energy and forces converged to 10^{-4} eV and 0.02 eV/Å, respectively. We used Grimme's empirical correction approach (GGA-D3) to correctly characterize the impact of the van der Waals interaction.[23]

DFT underestimates the bandgap because of the self-interaction error.[24–27] In previous work,[16] we confirmed that HSE with $\alpha = 0.05$ gives a bandgap (1.962 eV) that is more consistent with the experimental value (1.96 eV) than is the bandgap obtained by GGA-PBE (Perdew–Burke–Ernzerhof generalized gradient approximation) (1.66 eV).[13] In the HSE calculation, the direct bandgap remains at the Γ point, similar to the GGA-PBE calculation. The HSE-derived lattice parameter for monolayer C_2N ($a = |\vec{a}| = |\vec{b}|$) is 8.317 Å, which is slightly lower than that the GGA-PBE value of 8.330 Å because of a strong localized wave function in the HSE calculation. As with monolayer graphene, the application of a perpendicular external electric field (up to 2 V/nm) to the C_2N monolayer does not change its bang gap.

From here on, we report the DFT results with HSE ($\alpha = 0.05$) and with the empirical correction method proposed by Grimme (GGA-D3). Recent work[16] shows that C_2N can form four different bilayer configurations with relatively low energy, labeled AA-, AB-, AB′-, and Min-stacking, as shown in Fig. 1.

Table I compares the computed lattice constant $a = |a| = |b|$, the interlayer distance h_0, the in-plane covalent bond lengths, the relative energies ΔE, and the energy gap E_g of each stacking configuration in bilayer C_2N. In all cases, the lattice constant and the interlayer distance are slightly smaller than those from the previous GGA + PBE calculation.[16] The larger interlayer distance in AA-stacking is attributed to the strong repulsion arising from C atoms, which are exactly above and below each other. Nonetheless, the in-plane covalent bond lengths C–N, C–C^1, and C–C^2 do not differ much between the configurations. The most favorable stacking is Min-stacking, which gives 18.149, 2.132, and 5.295 meV/atom less than AA-, AB-, and AB′-stacking, respectively. This stability order is similar to that obtained previously from a GGA-PBE calculation.[16]

The electronic band structure of different bilayer configurations is shown in Figs. S1(a)–S1(d) in the supplementary material. As with the C_2N monolayer, all bilayer configurations have a direct bandgap at the Γ point. The AB-stacking arrangement has the largest bandgap of

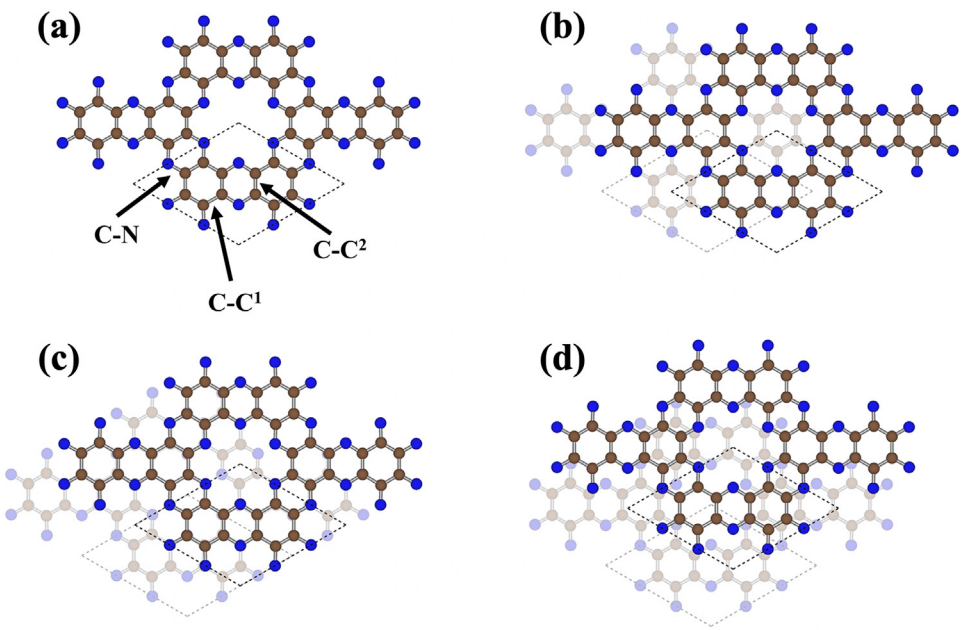


FIG. 1. (a)–(d) 2×2 supercell bilayer C_2N configurations with AA-, AB-, AB′-, and Min-stacking, respectively. Carbon and nitrogen atoms are represented as blue and brown balls, respectively.

Published under an exclusive license by AIP Publishing

TABLE I. The computed lattice constant a, interlayer distance h_0, in-plane covalent bond length, relative energies ΔE, and energy gap E_g of C_2N bilayer with different stacking configurations.

	Min	AA	AB	AB′
a (Å)	8.317	8.317	8.317	8.317
h_0 (Å)	3.081	3.414	3.131	3.186
C–N (Å)	1.334	1.334	1.334	1.335
$C–C^1$ (Å)	1.468	1.468	1.468	1.468
$C–C^2$ (Å)	1.427	1.427	1.427	1.427
ΔE (meV/atom)	0	18.149	2.132	5.295
E_g (eV)	1.582	1.354	1.630	1.305

1.630 eV, whereas the Min-, AA-, and AB′-stacking configurations have bandgaps of 1.582, 1.354, and 1.305 eV, respectively (Table I).

The van der Waals interaction in the multi-layer system is known to be an important factor in describing the electronic structure of 2D materials. Previous work[16] shows that different van der Waals correction methods (GGA + D2, GGA + D3, HSE + D3, and SCAN + rVV10) yield the same conclusion regarding the stability. Herein, we use HSE and the empirical correction method proposed by Grimme (HSE + D3) to obtain an accurate description of the effect of the van der Waals interaction.

Figure 2 shows the bandgap modification of the four configurations by a perpendicular external electric field of magnitude up to 4 V/nm. The direct bandgap characteristic of all four configurations is maintained. In all situations, the bandgap decreases monotonically as the electric-field strength increases. This is in sharp contrast with bilayer graphene, where the bandgap increases with increasing electric-field strength.[28] The decreasing bandgap as a result of electric field effects of AA- and AB-stacking is consistent with the previous calculations of Bafekry *et al.*[29] and Zhang *et al.*,[14] respectively. According to Fig. 2, the decreasing bandgap of bilayer C_2N can be sorted into two groups: Min- and AB′- vs the AA- and AB-configuration. This result suggests that interlayer interactions affect the electric-field-induced bang-gap modulation. Recall that, for the Min- and AB-configurations, all N atoms in the upper layer do not directly stack on C atoms in the bottom layer, as shown in Fig. 1. Conversely, in the AA- and AB-configurations, all N atoms in the upper layer are right on top of the C atoms in the lower layer. In a supporting manner (see Fig. S2 in the supplementary material), we analyze the partial charge density of the valence-band maximum (VBM) and the conduction-band minimum (CBM) of each configuration. In the case of Min- and AB′-configurations, the CBM has contributions from by p_x, p_y, and p_z from both C and N atoms, as shown in Figs. S2(g)–S2(h) in the supplementary material. However, for the AA- and AB-configurations, only the p_z charge orbital of N atoms contributes to the CBM, as shown in Figs. S2(e) and S2(f) in the supplementary material.

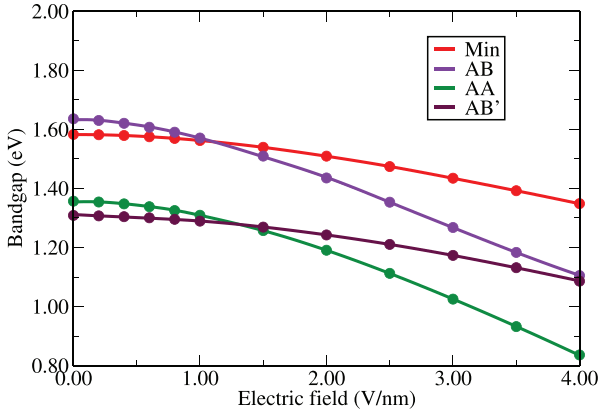


FIG. 2. Bandgap modulation of Min-, AA-, AB-, and AB′-stacking bilayer C_2N with an external electric field. The red, purple, green, and brown lines represent Min-, AB-, AA-, and AB′-stacking, respectively.

We further calculate the band structures of Min-C_2N under 0, 1, 2, 3, and 4 V/nm external electric fields (see Fig. 3, where the deep N-s states have been aligned to the same energy). All bands are rather stable in the conduction band, which contrasts with the blueshift with increasing electric-field strength in the valence band. A close inspection of the valence band indicates that the nitrogen p_x and p_y states shift closer to the p_z state upon increasing the electric-field strength. This finding results in a flattening of the VBM, which is known as the Stark effect.[30–33] The valence and conduction subband states separately mix, which results in a field-induced splitting of electronic levels. Accordingly, the valence- and conduction-band states are modulated by the electric-field strength. A similar result is also reported for single-walled boron nitride nanotubes, nanoribbons, and MoS_2 bilayers.[34–38] This resemblance to the atomic-level Stark effect leads to what is called "the giant Stark effect" by Khoo and Louie.[34]

Strain can potentially modulate the bandgap of 2D materials. Accordingly, we also investigate how perpendicular tensile and compressive strain affect the bandgap of the Min-configuration via the HSE + D3 calculation. Starting from the equilibrium interlayer distance h_0 of 3.081 Å, the tensile strain leads to the interlayer expansion, while the compressive strain leads to the interlayer contraction. Unlike bilayer graphene,[39,40] the bilayer C_2N preserves the direct bandgap

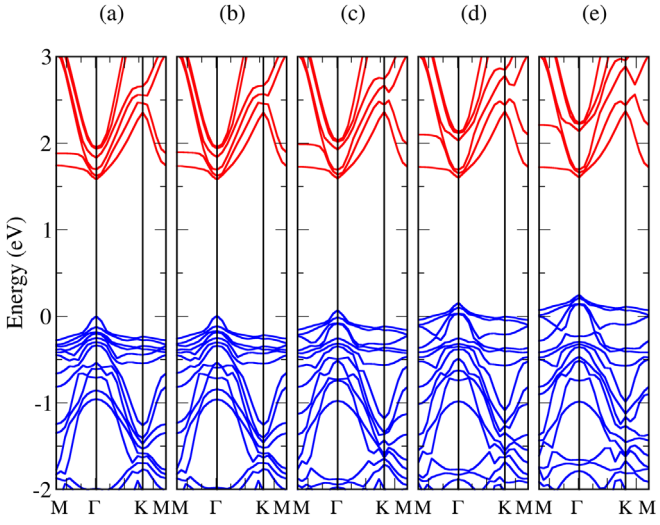


FIG. 3. (a)–(e) Band structure of Min-configuration bilayer C_2N with external electric field of 0, 1, 2, 3, and 4 V/nm, respectively.

Published under an exclusive license by AIP Publishing

even under strain. Figure 4 shows that the bandgap varies in parallel with the interlayer distance. Notably, the bandgap slowly increases with tensile strain but rapidly decreases with compressive strain. This result contrasts with bilayer graphene,[2,39,40] where the bandgap is insensitive to strain.

Pressure can be converted continuously after the magnitude interlayer change.[19] Next, the calculated total energy is fit to the stabilized jellium equation of state equation,[41]

$$E(V) = \frac{x_0}{(V/V_0)} + \frac{x_1}{(V/V_0)^{2/3}} + \frac{x_2}{(V/V_0)^{1/3}} + x_3, \quad (1)$$

where V is the volume of the cell under strain, V_0 is the equilibrium volume, and x_0, x_1, x_2, and x_3 are the fitting parameters. In our system, the volume V is the product of the planar area $A = |\vec{a} \times \vec{b}|$ and the interlayer distance h_0. The constants x_0, x_1, x_2, x_3, and V_0 are specific to the supercell size of 2×2 in Min-configuration C_2N. It is found that these numerical parameters are $x_0 = 1674.026$, $x_1 = -4785.939$, $x_2 = 4549.800$, and $x_3 = -1764.775$ and the equilibrium volume $V_0 = 185.56$ Å^3. This provides the continuous variation of pressure (P in GPa) as a function of volume (V in Å^3) as

$$P[\text{GPa}] = \frac{x_0' V_0}{V^2} + \frac{x_1' V_0^{2/3}}{V^{5/3}} + \frac{x_2' V_0^{1/3}}{V^{1/3}}, \quad (2)$$

where x_0', x_1', and x_2' are 2.682×10^5, -5.112×10^5, and 2.430×10^5, respectively. The calculated pressure of strained Min-C_2N as a function of the interlayer distance can be obtained by this equation and is plotted in Fig. 4. The bandgap decreases from 1.75 to 0.9 eV upon applying a pressure of 35 GPa. A pressure increase in up to 2.5 GPa produced by a hydraulic press was reported for a hBN-encapsulated graphene device.[19] In addition, a typical diamond anvil cell could produce a pressure of 100 GPa.[42,43] Thus, the bandgap modulation by pressure in bilayer C_2N merits further experimental study.

Finally, we show how the combination of strain and electric field affect the bandgap of Min-C_2N. Starting at the equilibrium of $h_0 = 3.08$ Å, we apply tensile (compressive) strain such that the interlayer distance increases (decreases) by 4% to 3.20 Å (2.80 Å). The applied electric field is up to 4 V/nm. The strained Min-configuration maintains the direct bandgap. Figure 5 shows that, under tensile strain, the bandgap rapidly decreases with increasing electric field, which is very similar to the result for strain-free Min-C_2N. Meanwhile, the bandgap slowly decreases with increasing electric field under compressive strain. In the latter case, unfortunately, the bandgap modulation of a few tens of eV is rather small and insufficient to develop nanoscale electronic devices.

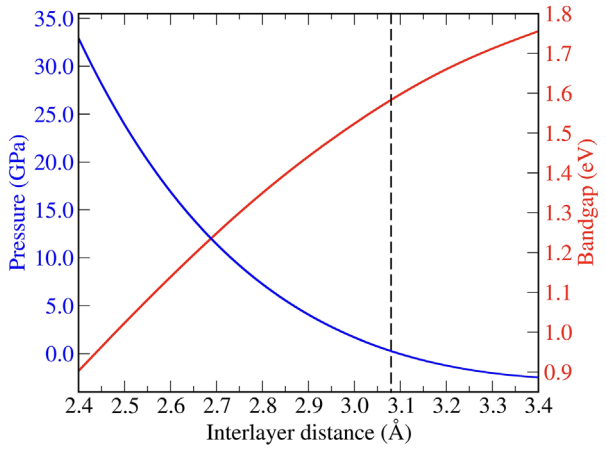


FIG. 4. The variation of pressure and bandgap of strained Min-C_2N as a function of the interlayer distance without an external electric field. The blue and red curves represent the pressure and bandgap, respectively. The dashed line divides the region of compressive strain (left side) from the region of tensile strain (right side).

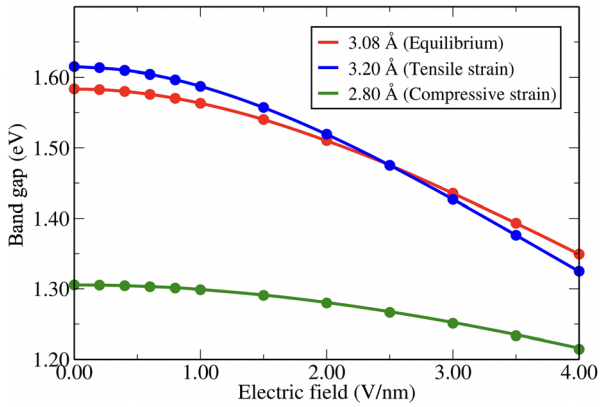


FIG. 5. Bandgap modulation of strained Min-stacking bilayer C_2N with an external electric field. The red curve represents the Min-stacking bilayer without strain. The blue and green curves represent the Min-stacking bilayer with tensile and compressive strain, respectively.

In summary, we have carried out first-principles calculations with the HSE functional to analyze the strain effect of bilayer C_2N with and without an external electric field of magnitude up to 4 V/nm. At equilibrium, strain-free interlayer distance, the bandgap of all four energetically favorable configurations decreases monotonically with increasing electric-field strength. Taking Min-C_2N as representative, the bandgap under zero electric field rapidly decreases with increasing compressive strain but slowly decreases with increasing tensile strain. We suggest that both strain engineering and the external electric field are potential candidates for experimentally tuning the bandgap of bilayer C_2N. This conclusion is also supported by the relation between strain (or the interlayer distance) and physical pressure using the stabilized jellium equation of state.

See the supplementary material for the band structures of all stacking as well as the wave-function localization for their VBM and CBM.

This work was supported by (i) the Suranaree University of Technology (SUT), (ii) the Thailand Science Research and Innovation (TSRI), and (iii) the National Science, Research and Innovation Fund (NSRF). K.D. was supported by the National Research Council of Thailand (NRCT) under No. NRCT5-RGJ63002-028. P.R. acknowledges the Thailand Research Fund (Grant No. RSA6280068) and the Kasetsart University Research and Development Institute (KURDI). We wish to thank the high-performance computing facilities at the King Mongkut's

Published under an exclusive license by AIP Publishing

University of Technology Thonburi (KMUTT, Thailand) for their hospitality.

AUTHOR DECLARATIONS

Conflict of Interest

The authors have no conflicts to disclose.

DATA AVAILABILITY

The data that support the findings of this study are available within the article and its supplementary material.

REFERENCES

[1]G. Giovannetti, P. A. Khomyakov, G. Brocks *et al.*, "Substrate-induced band gap in graphene on hexagonal boron nitride: *Ab initio* density functional calculations," Phys. Rev. B **76**, 073103 (2007).

[2]S.-M. Choi, S.-H. Jhi, and Y.-W. Son, "Effects of strain on electronic properties of graphene," Phys. Rev. B **81**, 081407 (2010).

[3]K. Nakada, M. Fujita, G. Dresselhaus *et al.*, "Edge state in graphene ribbons: Nanometer size effect and edge shape dependence," Phys. Rev. B **54**, 17954 (1996).

[4]J. Zhou, M. M. Wu, X. Zhou *et al.*, "Tuning electronic and magnetic properties of graphene by surface modification," Appl. Phys. Lett. **95**, 103108 (2009).

[5]Z. Ao and F. Peeters, "Electric field activated hydrogen dissociative adsorption to nitrogen-doped graphene," J. Phys. Chem. C **114**, 14503–14509 (2010).

[6]E. McCann and V. I. Fal'ko, "Landau-level degeneracy and quantum Hall effect in a graphite bilayer," Phys. Rev. Lett. **96**, 086805 (2006).

[7]E. McCann, "Asymmetry gap in the electronic band structure of bilayer graphene," Phys. Rev. B **74**, 161403 (2006).

[8]J. B. Oostinga, H. B. Heersche, X. Liu *et al.*, "Gate-induced insulating state in bilayer graphene devices," Nat. Mater. **7**, 151–157 (2008).

[9]R. B. dos Santos, F. de Brito Mota, R. Rivelino *et al.*, "Electric-field control of spin-polarization and semiconductor-to-metal transition in carbon-atom-chain devices," J. Phys. Chem. C **121**, 26125–26132 (2017).

[10]X. Gao, Z. Zhou, Y. Zhao *et al.*, "Comparative study of carbon and BN nanographenes: Ground electronic states and energy gap engineering," J. Phys. Chem. C **112**, 12677–12682 (2008).

[11]L. Li, Y. Yu, G. J. Ye *et al.*, "Black phosphorus field-effect transistors," Nat. Nanotechnol. **9**, 372 (2014).

[12]B. Radisavljevic, A. Radenovic, J. Brivio *et al.*, "Single-layer MOS_2 transistors," Nat. Nanotechnol. **6**, 147 (2011).

[13]J. Mahmood, E. K. Lee, M. Jung *et al.*, "Nitrogenated holey two-dimensional structures," Nat. Commun. **6**, 6486 (2015).

[14]R. Zhang, B. Li, and J. Yang, "Effects of stacking order, layer number and external electric field on electronic structures of few-layer C_2N-*h*2D," Nanoscale **7**, 14062–14070 (2015).

[15]R. Longuinhos and J. Ribeiro-Soares, "Stable holey two-dimensional C_2N structures with tunable electronic structure," Phys. Rev. B **97**, 195119 (2018).

[16]K. Dabsamut, T. Jiraroj, S. Jungthawan *et al.*, "Stacking stability of C_2N bilayer nanosheet," Sci. Rep. **9**, 6861 (2019).

[17]A. Kakanakova-Georgieva, G. K. Gueorguiev, D. G. Sangiovanni *et al.*, "Nanoscale phenomena ruling deposition and intercalation of AlN at the graphene/SiC interface," Nanoscale **12**, 19470–19476 (2020).

[18]A. Kakanakova-Georgieva, F. Giannazzo, G. Nicotra *et al.*, "Material proposal for 2D indium oxide," Appl. Surf. Sci. **548**, 149275 (2021).

[19]B. L. Chittari, N. Leconte, S. Javvaji *et al.*, "Pressure induced compression of flatbands in twisted bilayer graphene," Electron. Struct. **1**, 015001 (2018).

[20]G. Kresse and J. Furthmüller, "Efficiency of ab-initio total energy calculations for metals and semiconductors using a plane-wave basis set," Comput. Mater. Sci. **6**, 15–50 (1996).

[21]G. Kresse and J. Furthmüller, "Efficient iterative schemes for *ab initio* total-energy calculations using a plane-wave basis set," Phys. Rev. B **54**, 11169 (1996).

[22]J. P. Perdew, K. Burke, and M. Ernzerhof, "Generalized gradient approximation made simple," Phys. Rev. Lett. **77**, 3865 (1996).

[23]S. Grimme, J. Antony, S. Ehrlich *et al.*, "A consistent and accurate *ab initio* parametrization of density functional dispersion correction (DFT-D) for the 94 elements H-Pu," J. Chem. Phys. **132**, 154104 (2010).

[24]J. L. Bao, L. Gagliardi, and D. G. Truhlar, "Self-interaction error in density functional theory: An appraisal," J. Phys. Chem. Lett. **9**, 2353–2358 (2018).

[25]P. Mori-Sánchez, A. J. Cohen, and W. Yang, "Many-electron self-interaction error in approximate density functionals," J. Chem. Phys. **125**, 201102 (2006).

[26]A. J. Cohen, P. Mori-Sánchez, and W. Yang, "Development of exchange-correlation functionals with minimal many-electron self-interaction error," J. Chem. Phys. **126**, 191109 (2007).

[27]V. Polo, E. Kraka, and D. Cremer, "Electron correlation and the self-interaction error of density functional theory," Mol. Phys. **100**, 1771–1790 (2002).

[28]H. Raza and E. C. Kan, "Field modulation in bilayer graphene band structure," J. Phys.: Condens. Matter **21**, 102202 (2009).

[29]A. Bafekry, C. Stampfl, M. Ghergherehchi *et al.*, "A first-principles study of the effects of atom impurities, defects, strain, electric field and layer thickness on the electronic and magnetic properties of the C_2N nanosheet," Carbon **157**, 371–384 (2020).

[30]A. Ramasubramaniam, D. Naveh, and E. Towe, "Tunable band gaps in bilayer transition-metal dichalcogenides," Phys. Rev. B **84**, 205325 (2011).

[31]J. Kim, S. S. Baik, S. H. Ryu *et al.*, "Observation of tunable band gap and anisotropic Dirac semimetal state in black phosphorus," Science **349**, 723–726 (2015).

[32]D. A. Miller, D. Chemla, T. Damen *et al.*, "Band-edge electroabsorption in quantum well structures: The quantum-confined stark effect," Phys. Rev. Lett. **53**, 2173 (1984).

[33]X. Lu and L. Yang, "Stark effect of doped two-dimensional transition metal dichalcogenides," Appl. Phys. Lett. **111**, 193104 (2017).

[34]K. Khoo and S. G. Louie, "Tuning the electronic properties of boron nitride nanotubes with transverse electric fields: A giant dc stark effect," Phys. Rev. B **69**, 201401 (2004).

[35]M. Ishigami, J. D. Sau, S. Aloni *et al.*, "Observation of the giant stark effect in boron-nitride nanotubes," Phys. Rev. Lett. **94**, 056804 (2005).

[36]C.-H. Park and S. G. Louie, "Energy gaps and stark effect in boron nitride nanoribbons," Nano Lett. **8**, 2200–2203 (2008).

[37]Z. Zhang, W. Guo, and B. I. Yakobson, "Self-modulated band gap in boron nitride nanoribbons and hydrogenated sheets," Nanoscale **5**, 6381–6387 (2013).

[38]Q. Liu, L. Li, Y. Li *et al.*, "Tuning electronic structure of bilayer MOS_2 by vertical electric field: A first-principles investigation," J. Phys. Chem. C **116**, 21556–21562 (2012).

[39]B. Nanda and S. Satpathy, "Strain and electric field modulation of the electronic structure of bilayer graphene," Phys. Rev. B **80**, 165430 (2009).

[40]B. Verberck, B. Partoens, F. Peeters *et al.*, "Strain-induced band gaps in bilayer graphene," Phys. Rev. B **85**, 125403 (2012).

[41]A. B. Alchagirov, J. P. Perdew, J. C. Boettger *et al.*, "Reply to 'comment on 'energy and pressure versus volume: Equations of state motivated by the stabilized jellium model' '," Phys. Rev. B **67**, 026103 (2003).

[42]A. Dewaele, P. Loubeyre, F. Occelli *et al.*, "Toroidal diamond anvil cell for detailed measurements under extreme static pressures," Nat. Commun. **9**, 2913 (2018).

[43]B. Li, C. Ji, W. Yang *et al.*, "Diamond anvil cell behavior up to 4 mbar," Proc. Natl. Acad. Sci. **115**, 1713–1717 (2018).

Published under an exclusive license by AIP Publishing